Long-term dopamine neurochemical monitoring in primates

Citation: Schwerdt, Helen N. et al. "Long-Term Dopamine Neurochemical Monitoring in Primates." Proceedings of the National Academy of Sciences 114, 50 (November 2017): 13260–13265 © 2017 The Authors

As Published: http://dx.doi.org/10.1073/PNAS.1713756114

Publisher: National Academy of Sciences (U.S.)

Persistent URL: http://hdl.handle.net/1721.1/117085

Version: Final published version: final published article, as it appeared in a journal, conference proceedings, or other formally published context

Long-term dopamine neurochemical monitoring in primates

Helen N. Schwerdt[a,b,c], Hideki Shimazu[a,b], Ken-ichi Amemori[a,b], Satoko Amemori[a,b], Patrick L. Tierney[a,b], Daniel J. Gibson[a,b], Simon Hong[a,b], Tomoko Yoshida[a,b], Robert Langer[c,d], Michael J. Cima[c,e], and Ann M. Graybiel[a,b,1]

[a]McGovern Institute for Brain Research, Massachusetts Institute of Technology, Cambridge, MA 02139; [b]Department of Brain and Cognitive Sciences, Massachusetts Institute of Technology, Cambridge, MA 02139; [c]Koch Institute for Integrative Cancer Research, Massachusetts Institute of Technology, Cambridge, MA 02139; [d]Department of Chemical Engineering, Massachusetts Institute of Technology, Cambridge, MA 02139; and [e]Department of Materials Science and Engineering, Massachusetts Institute of Technology, Cambridge, MA 02139

Contributed by Ann M. Graybiel, November 1, 2017 (sent for review August 4, 2017; reviewed by Richard Courtemanche, Paul W. Glimcher, and Christopher I. Moore)

Many debilitating neuropsychiatric and neurodegenerative disorders are characterized by dopamine neurotransmitter dysregulation. Monitoring subsecond dopamine release accurately and for extended, clinically relevant timescales is a critical unmet need. Especially valuable has been the development of electrochemical fast-scan cyclic voltammetry implementing microsized carbon fiber probe implants to record fast millisecond changes in dopamine concentrations. Nevertheless, these well-established methods have only been applied in primates with acutely (few hours) implanted sensors. Neurochemical monitoring for long timescales is necessary to improve diagnostic and therapeutic procedures for a wide range of neurological disorders. Strategies for the chronic use of such sensors have recently been established successfully in rodents, but new infrastructures are needed to enable these strategies in primates. Here we report an integrated neurochemical recording platform for monitoring dopamine release from sensors chronically implanted in deep brain structures of nonhuman primates for over 100 days, together with results for behavior-related and stimulation-induced dopamine release. From these chronically implanted probes, we measured dopamine release from multiple sites in the striatum as induced by behavioral performance and reward-related stimuli, by direct stimulation, and by drug administration. We further developed algorithms to automate detection of dopamine. These algorithms could be used to track the effects of drugs on endogenous dopamine neurotransmission, as well as to evaluate the long-term performance of the chronically implanted sensors. Our chronic measurements demonstrate the feasibility of measuring subsecond dopamine release from deep brain circuits of awake, behaving primates in a longitudinally reproducible manner.

striatum | voltammetry | neurotransmitters | chronic implants

Dopamine neurotransmission is central to movement, motivation, and behavioral choice, along with other fundamental behaviors (1, 2). Dysregulation of dopamine occurs in neuropsychiatric and neurologic disorders, including major depression and Parkinson's disease, impairing quality of life on a daily basis (3, 4). Methods to allow accurate in vivo monitoring of dopamine over extended timescales still have not been technically feasible for primate brains, however, preventing the possibility of assessing longitudinally the role of this neurotransmitter in neurodegeneration and in the modulation of behavior.

Electrochemical fast-scan cyclic voltammetric (FSCV) techniques have been shown to provide the optimal overall performance for measuring dopamine neurotransmission at the required fast timescales (milliseconds), sensitivity (nanomolar), and chemical selectivity. Most such measurements, for technical reasons, have been made from acutely implanted sensors that provide a sensitive, minimally scarring interface. Chronic dopamine recording systems have only begun to gain widespread use (1, 2), and these methods have so far been applied only to rodents. There is a great need to establish chronic measurements in primates, for whom to date there are only few reports even of acute dopamine measurements (5–8), with stable measurements only for a few hours. The lack of chronic chemical sensors exists despite great progress in the chronic electrophysiological recording of spike and local field potential activity in behaving nonhuman primates. Chronic measurements of dopamine will aid in the identification of dopamine's contribution to complex behaviors degraded in human disorders, and to aid in testing the clinical feasibility of treatments. Specific hurdles have included large size, increasing the likelihood of tissue damage and probe degradation, and the lack of infrastructure to allow physical probe stability with on-demand movability.

Key challenges associated with the chronic use of FSCV derive from the degraded capacity of long-implanted sensors to detect dopamine due to both biologic and nonbiologic processes (9). Neurochemical measurements made from acutely implanted sensors produce minimal scarring due to brevity of contact (i.e., interface for several hours). Chronically implanted sensors, however, produce persistent inflammation and scarring around the sensor, which effectively produces a barrier between the sensor and regions of neurochemical release. The carbon fiber (CF) sensors used for FSCV semipermanently adsorb and accumulate films of proteins and byproducts of neurotransmitter redox reactions (10), all of which are amplified by inflammation (9). Implant size reductions have been critical to minimize

Significance

Dopamine is an important neurotransmitter governing behavior and heavily implicated in a large range of neural disorders, including Parkinson's disease, depression, and related mood and movement disorders. Methods allowing accurate monitoring of dopamine over long timescales have not been previously reported yet are crucial to enable improved diagnostics and therapeutics. We report a technical advance that allowed recording of dopamine from sensors implanted into the brains of nonhuman primates for over 100 days. Our integrated platform enabled monitoring fast changes in dopamine release in response to rewarding stimuli and the administration of dopamine-related drugs. These findings demonstrate the long-term feasibility and reproducibility of neurochemical measurements and strengthen their potential translation to human use.

Author contributions: H.N.S., H.S., K.-i.A., R.L., M.J.C., and A.M.G. designed research; H.N.S., H.S., K.-i.A., P.L.T., S.H., and A.M.G. performed research; H.N.S., S.A., D.J.G., T.Y., and A.M.G. analyzed data; and H.N.S., H.S., and A.M.G. wrote the paper.

Reviewers: R.C., Concordia University; P.W.G., New York University; and C.I.M., Brown University.

The authors declare no conflict of interest.

[1]To whom correspondence should be addressed. Email: graybiel@mit.edu.

This article contains supporting information online at www.pnas.org/lookup/suppl/doi:10.1073/pnas.1713756114/-/DCSupplemental.

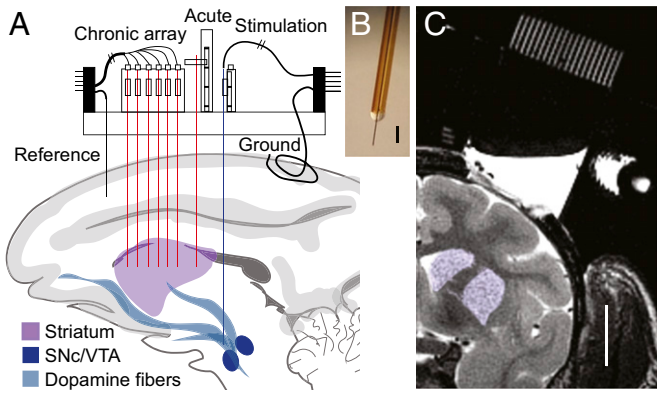

Fig. 1. Modular platform for chronic neurochemical measurements. (*A*) Modular chamber combines usage of acute and chronic systems and targets multiple widespread brain regions. (*B*) Primate-implantable CF sensor. (Scale bar, 100 μm.) (*C*) MRI of chamber grid and targeted striatal sites (purple). (Scale bar, 1 cm.)

brain response (9, 11) and to provide stable long-term use in rodents (1, 2).

We have developed for nonhuman primate use sensors that maintain the small rodent-scale footprints (1, 2) (7-μm tip diameter), and we have implemented these in macaque monkeys outfitted with a modular chamber interface (12) (Fig. 1 and Fig. S1), allowing us to introduce CF sensors and to measure from these probes both acutely and chronically. This modular implant platform allowed us to make measurements of dopamine release from multiple sites in the striatum [the caudate nucleus (CN) and the putamen], as well as to identify and manipulate dopamine-containing brain regions [substantia nigra pars compacta (SNc) and ventral tegmental area (VTA)] that give rise to striatal dopamine-containing inputs. We measured dopamine release in response to direct, controllable electrical and pharmacologic stimulation, as well as behavior-related and spontaneous dopamine release from the awake monkeys for over months-long time periods. We characterized in detail the performance of the chronically implanted sensors in acute recordings as well to validate the identification of dopamine, and in chronic recordings to test the capacity of our probes to measure dopamine reliably for up to 170 d.

Results and Discussion

Following classic acute FSCV methods (1, 2), we measured striatal dopamine release induced by direct electrical stimulation of SNc-VTA cells and fibers and by systemic administration of a dopamine-releasing drug (raclopride) to characterize performance of chronically implanted sensors. Stimulation electrodes were implanted to target the SNc-VTA as estimated by MRI with our modular chamber (Fig. 1*C* and Fig. S1). Positions of the stimulating electrodes were optimized by recording neuronal spike activity predictive of reward (13) during behavioral performance or by directly measuring stimulation-induced dopamine from sensors acutely implanted in the striatum.

We first measured electrically stimulated striatal dopamine release from chronically implanted sensors (Fig. 2 and Fig. S2). The chemical identities of the measured electrochemical currents were evaluated by the shape of their cyclic voltammograms (CVs), which demonstrated distinctive current peaks at the dopamine redox potentials of ~−0.2 and 0.6 V (Fig. 2*B*). These measurements were corroborated by administering raclopride (dopamine D2 receptor antagonist), which increased the amount of stimulation-evoked dopamine as measured from chronic sensors (151% increase, $P < 0.0005$, six sites in four sessions, in monkey M1) (Fig. 2 *C*–*E*). We confirmed that these effects could also be obtained from acute sensors (149% increase, $P = 0.028$, from four sites in four sessions in monkeys M1, M2, and M3) (Fig. 2*E* and Fig. S3). The raclopride administration not only increased stimulation-induced release, but could also be used to increase spontaneous dopamine neurotransmission. This drug was used to monitor and to modulate reproducibly endogenous dopamine neurotransmission.

We developed an automated algorithm to identify these transient changes in apparent dopamine concentration ($[DA]_a$) (Fig. 3) to detect such spontaneous dopamine release over extended periods of recording from the chronically implanted sensors. The

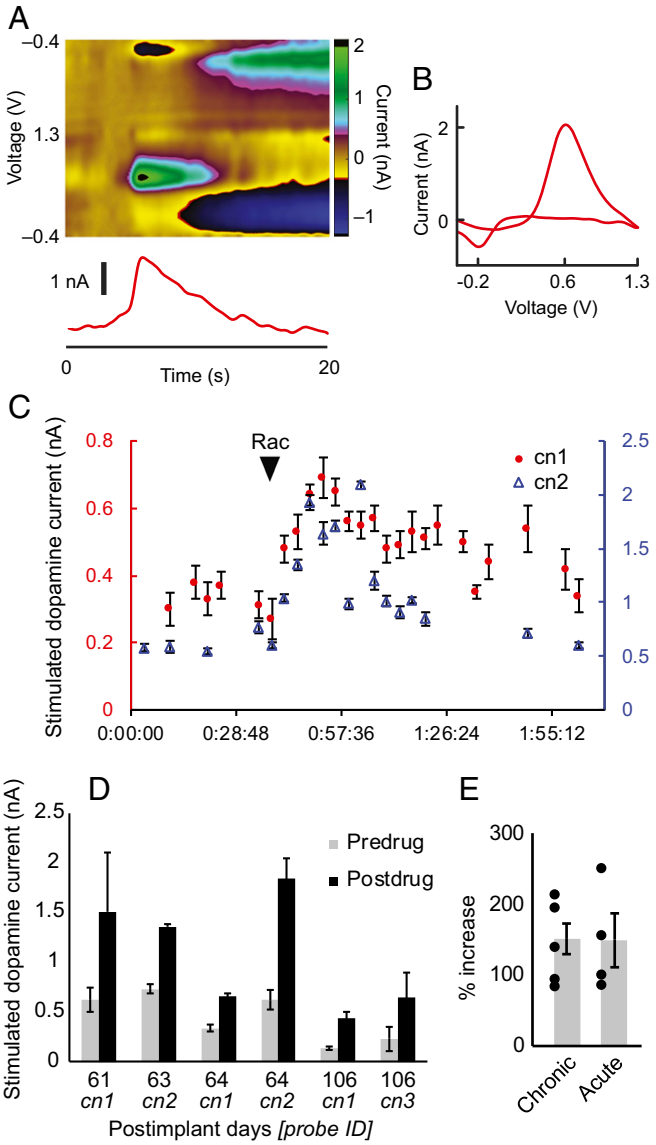

Fig. 2. Chronic measurements of dopamine release evoked by electrical stimulation in monkey M1. (*A*) Electrical stimulation-evoked dopamine measured on postimplant day 61 (probe cn1) in M1. (*B*) CV conferring dopamine neurochemical identity of measurement in *A*. (*C*) Stimulation-induced dopamine oxidation current over time recorded from two electrodes (cn1 and cn2) on postimplant day 64 in M1. Raclopride (Rac; arrowhead) increases dopamine release. (*D*) Average peak stimulation-evoked dopamine measured from chronically implanted sensors (cn1–3) before and after raclopride drug treatment on postimplant days 61, 63, 64, and 106 in M1. Error bars represent SD. (*E*) Percent increase of stimulated-evoked dopamine following drug treatment for chronic (from five sites in M1, see Table S1) and acute measurements (from four sites in M1, M2, and M3). Error bars represent SEM.

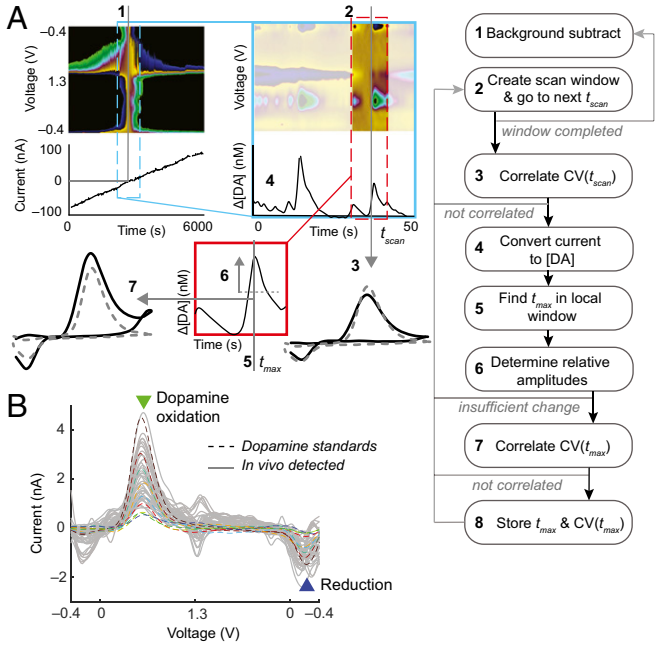

Fig. 3. Automated detection of dopamine. (*A*) Flow-chart diagram of developed algorithm used to identify local increases in dopamine (i.e., transients). Specific procedures are also detailed in *Materials and Methods*. (*B*) Representative CVs (gray) automatically extracted from a recording in ventral CN (cl6) of monkey M2 on postimplant day 124, demonstrating distinctive peaks at dopamine redox potentials and tight correlation to in vitro dopamine standards (eight overlaid colored dashed traces).

boosting effects of raclopride were reliably tracked on spontaneous dopamine release with sensors implanted for over 4 mo (monkeys M1 and M2) (Fig. 4, Fig. S4, and Table S1), including tracking from multiple sites synchronously (Fig. S5). An increase in the rate of dopamine neurotransmission was observed following raclopride treatment from the chronic sensors (average change of 102% from 7 increases and 1 decrease in M1 and 11 increases and 4 decreases in M2, $P = 0.0183$) (Fig. 4 and Table S1). Nonsignificant changes in dopamine concentration were detected after raclopride (average increase of 5.8 nM in peak dopamine after treatment across 23 measurement sites, $P = 0.26$) (Fig. 4). We simultaneously monitored these types of changes as they occurred across multiple widely distributed regions across the CN and putamen in M2 (Fig. S5). All of these chronically measured drug-modulated dopamine dynamics could be confirmed with acute measurements made in separate sessions (Fig. S4).

We tested whether the chronic sensors could be used to measure striatal dopamine changes in response to rewarding (1, 2, 13) (Fig. 5 *A*–*C*) or surprising (14, 15) (Fig. 5*D*) stimuli. This goal was achieved with monkey M2 in 19 recording sessions and in M1 in 4 recording sessions made with sensors chronically implanted over 4–5 mo. We detected reproducible patterns of dopamine changes as M2 performed a reward-biased visual saccade task [also referred to as the one-direction reward (1DR) task] (16), which required the animal to fixate a central fixation point and then, once it was extinguished, to make leftward or rightward saccadic eye movements to a single peripherally illuminated target to receive, in different trials, small or large liquid rewards (Fig. 5 *E* and *F* and Figs. S6 and S7). Larger dopamine concentration changes were detected in trials that were associated with larger liquid rewards (Fig. 5 *E*–*G*), a result aligned with the results of electrophysiological recording of the spike activity of striatal neurons during similar motivational tasks in macaques (17). These single-session chronic implant measurements compared favorably with those that we recorded with acutely implanted sensors (Fig. S6).

Direct measurements of behaviorally important neurochemicals have been rare in primates and have only been made from acutely implanted sensors. Here we show the feasibility of these long-term recordings. The chronic dopamine monitoring methods that we introduce here were validated with direct stimulation, pharmacologic, and behavioral protocols. The introduction of such long time-scale recordings of dopamine release and their applications in monitoring behaviorally encoded and drug-modulated dopamine neurotransmission should open up the possibility of measuring dopamine dynamics during performance of complex tasks, a critical step toward understanding how dopamine signaling evolves during learning and motivationally influenced behaviors. As a prototype of such experiments, we used the 1DR task, well known as a task in which spike activity related to motivation can be interrogated (16). We show that in the same task that triggers these electrophysiological signals, dopamine release is triggered.

The extended monitoring that was provided by our integrated modular platform and algorithm could also be of great value in clinical settings. Such measurements could provide diagnostic measures of disease state and could be used to directly modify treatment schedules, including those for patients already implanted with deep brain stimulation devices, such as those implemented for Parkinson's disease therapy. These chronic measurements could simplify procedures for assessing the functional integrity of implanted sensors without the need for additional implants to stimulate directly the release of dopamine. Such procedures are impractical and risky in primates. The chronic implants could further supplant use of the stiffer stimulation electrodes used with conventional FSCV, which can physically shift position over time (18), resulting in varying the amount of stimulated striatal dopamine. Dopamine is heterogeneously released in the striatum (19–21), and this spatial heterogeneity is related to the activity of afferents in SNc/VTA. The multichannel probing capabilities introduced here could be useful for elaborating topographical midbrain projections to the striatum (22). The electrochemical interface design and measurement protocols that we introduce here for dopamine could be used broadly to detect chemical dynamics with long-term viability of neurochemical measurements.

Materials and Methods

Additional methods are provided in *SI Materials and Methods*.

Animals and Surgery. Two female rhesus macaque (*Macaca mulatta*) monkeys (M1, 6.5 kg, and M2, 9.8 kg) were studied for acute and chronic recording and one female rhesus macaque monkey (M3, 8.4 kg) was studied for acute recording. Monkeys M1 and M3 were used for immunohistochemistry to validate the location of implanted sensors and stimulation electrodes. All experimental procedures were approved by the Committee on Animal Care of the Massachusetts Institute of Technology. Monkeys were adapted to transitions from cages to primate chairs using pole-and-collar and food or liquid reinforcement. Animals were fitted with chronic chambers and grids (12) in successive surgeries (chamber implantation and craniotomy) performed under sterile conditions and with administration of sevoflurane anesthesia preceded by intramuscular administration of ketamine (10 mg/kg) and atropine (0.04 mg/kg). Postoperative maintenance included administration of buprenorphine (0.15–0.2 mg/kg, subcutaneously), dexamethasone (0.09–0.11 mg/kg, intramuscularly), ceftriaxone (1.2–1.6 mg/kg, intramuscularly), and famotidine (0.4–0.51 mg/kg, intramuscularly).

Modular Chamber Implant Platforms. Chambers for monkeys M1 and M3 were constructed as previously reported (12) and provided access for devices to be implanted to brain structures either on a day-by-day basis or chronically. Chambers were placed above the right hemisphere and in the coronal plane at angles of 4°, 23°, and 5°, respectively, for M1, M2, and M3. In M2, a smaller, single-hemisphere chamber (obtained from Gray Matter Research) was used (Fig. 1). Grids were installed within the chambers and consisted of an array of holes spaced 1-mm apart (40 × 30 or 24 × 20) having 1-mm center-to-center distance and 0.48- or 0.64-mm diameters (Fig. S1*A*). Anatomical targeting was

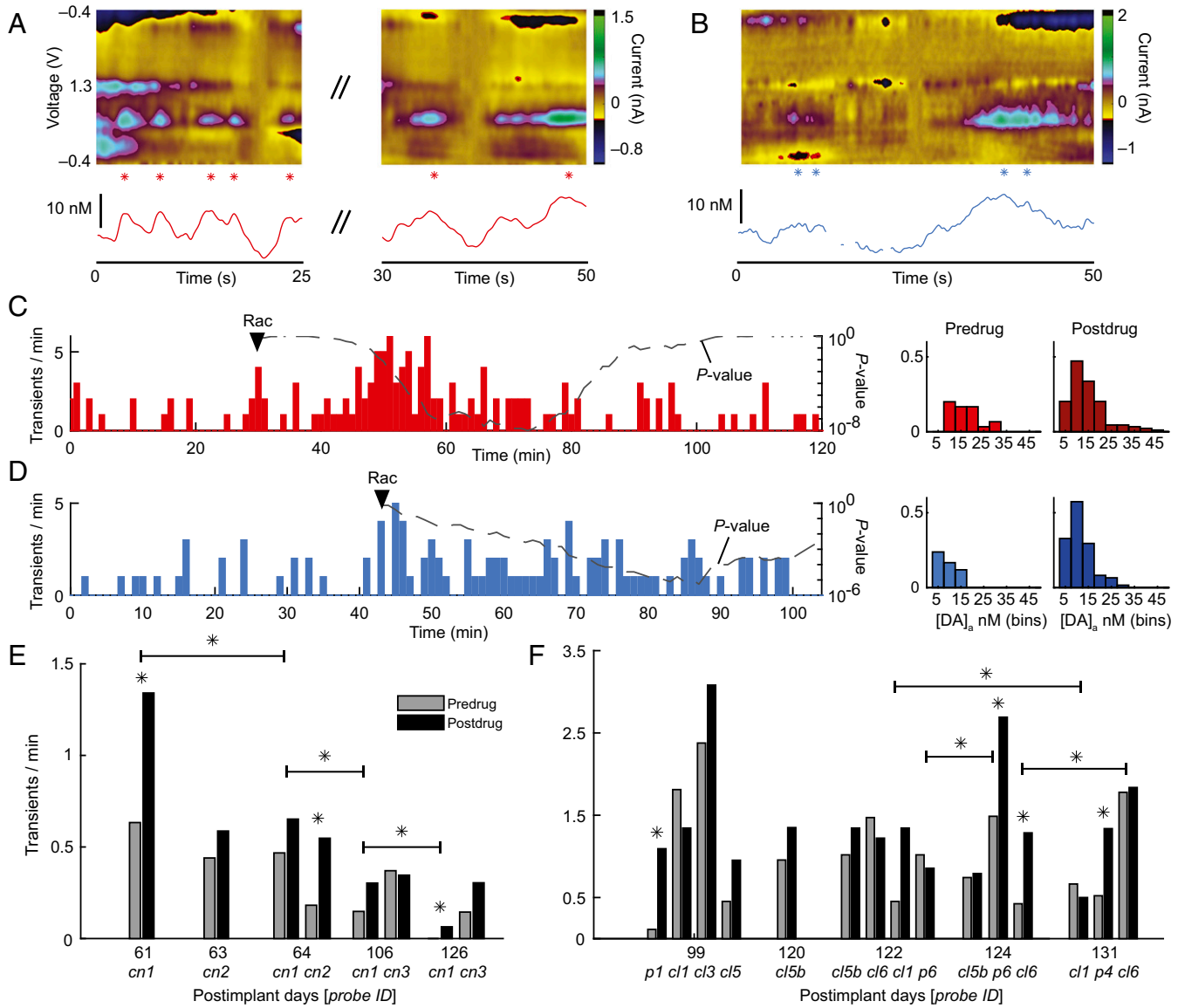

Fig. 4. Chronic measurements of drug-modulated dopamine neurotransmission using automated detection algorithms. (*A* and *B*) Representative endogenous dopamine transients after raclopride (Rac) treatment recorded in the CN of monkey M1 on postimplant day 61 (*A*) and in the putamen of M2 on postimplant day 131 (*B*). Asterisks denote detected dopamine transients. (*C*) The *Left* plot shows rate of detected dopamine transients (*Left y* axis) over time from a continuous recording in the same session shown in *A*. *Right y* axis indicates *P* value (dashed or dotted for increase or decrease, respectively, χ^2 test) for a sliding window equal to the baseline period (before arrowhead). Higher significance (lower *P* values) occurs as the postdrug rate increases above baseline rate. The *Right* plot is the distribution of detected dopamine concentration changes (before and after drug treatment) and their frequencies from rate data plotted at *Left*. (*D*) Same as *C* for the session represented in *B*. (*E* and *F*) Rates of detected dopamine measured over the course of recording sessions (postimplant days) in M1 (*E*) and M2 (*F*). *$P < 0.05$ (χ^2 test).

achieved by using structural 3.0T MRI (T1-weighted, 0.5-mm isotropic and T2-weighted, 0.35-mm isotropic) to allow measurements relative to grid-hole coordinates (Fig. S1*B*). Micromanipulators (MO-97A; Narishige) were mounted as needed onto chambers to allow acute implantation of sensors or stimulation electrodes (Fig. S1*C*). Microdrives (12) were permanently installed onto grids for fixing chronic devices (Fig. S1*D*). In all monkeys (M1–M3), CF sensors were acutely implanted into the CN and putamen to allow measurement of stimulation-evoked dopamine release. In M1, six CF sensors were chronically implanted into the CN and were fixed onto microdrive shuttles. In M2, 19 CF sensors were chronically implanted into the CN and putamen. See *SI Materials and Methods* for detailed implantation methods.

Electrochemical Recording. FSCV was performed using computer-controlled instrumentation that allowed synchronous recording from four channels. Each channel was connected to a CF sensor to apply a triangular voltage waveform (–0.4 to 1.3 to –0.4 V at 400 V/s scan rate and 10-Hz cycle frequency) and record generated current (see *SI Materials and Methods* for details).

Chemometric Analysis. The chemical identity of the measured electrochemical signals as being dopamine was conferred by analysis of the CVs of the background-subtracted data. Dopamine is known to produce current changes at reduction and oxidation (redox) potentials of –0.2 and 0.6 V, respectively, with the FSCV parameters applied in this work (2). Measured CVs were further analyzed against in vitro dopamine standards (nine CVs) generated in the flow cell to compute Pearson's correlation coefficient, *r*. Measured CVs were only identified as dopamine when *r* was greater than a threshold, r_t, as correlated to a dopamine standard and extraneous variance (*Q*, or residual sum of squares) was below a tolerance level (Q_α) during automated detection (see *Automated Dopamine Detection*).

Principal component regression (PCR) (19, 23) was used to convert background-subtracted electrochemical current to projected changes in apparent dopamine and also nondopamine currents (i.e., pH, background drift, and movement) based on the principal components provided (i.e., 9 dopamine standards, 8 pH standards, 11 background drift standards, and 36 movement standards) (*SI Materials and Methods*). The dopamine standards can be seen

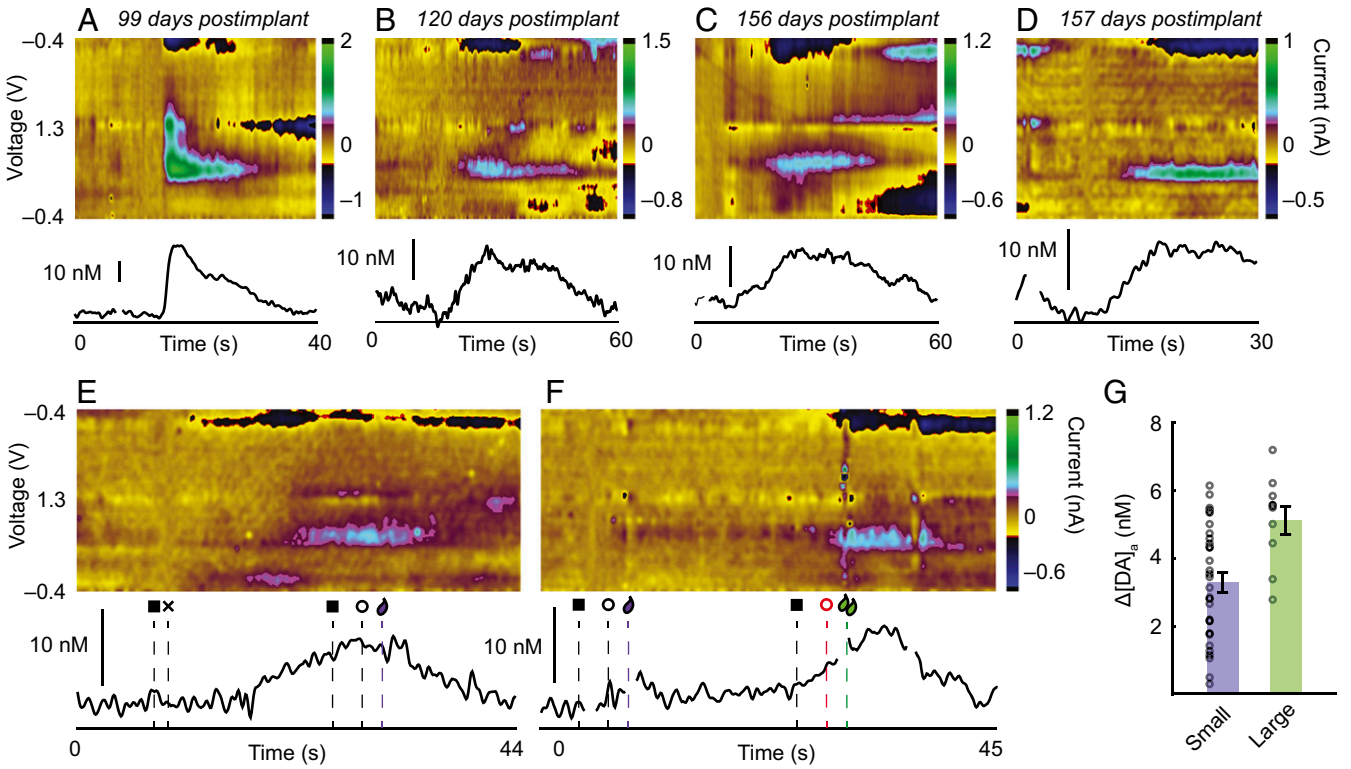

Fig. 5. Chronic measurements of behavior-related dopamine release. (*A*) Phasic dopamine increase with intake of sweet liquid reward, measured from dorsomedial putamen (p1 in monkey M2). (*B*) Dopamine increase in CN (cl5b in M2) after intake of sweet liquid. (*C*) Dopamine increase in CN (cn3 in M1) during delivery of sweet potato treat. (*D*) Representative dopamine increase in putamen (p3 in M2) after surprising closing of chamber door. (*E* and *F*) Dopamine changes in small (*E*) and large (*F*) reward trials in 1DR task (legend of event markers in Fig. S5). (*G*) Average dopamine concentration changes detected in small and large reward trials. For *E*–*G*, measurements were taken from ventral CN of M2 on postimplant day 131. Error bars show SE of mean.

overlaid with in vivo measurements in Fig. 3*B*. In vivo dopamine concentration changes were estimated based on in vitro calibrations. PCR-calculated projected dopamine current was converted to apparent dopamine concentration change ($\Delta[DA]_a$) by dividing it by the normalized sensitivity (19) (i.e., in vitro dopamine sensitivity in nanoampere per nanomolar relative to background current in nanoampere), and measured background current. CVs that could not be accounted for as a physiological signal were automatically blanked out if $Q \geq Q_\alpha = 21$. Only dopamine and pH standards were used to calculate the threshold, $Q_\alpha = 21$, to ensure that current contributions that did not fall within expected bounds of primary contributions with a confidence interval of 95% were removed from analysis. $\Delta[DA]_a$ traces were also nulled at points where CVs were found to be highly correlated ($r > 0.8$) to movement standards.

The correlation threshold, $r_t = 0.8$, was determined such that the hit rate (probability that measured dopamine signals were accurately identified as dopamine) was 92%; the miss rate (probability that dopamine signals were not identified) was 26%; and the rate of false positives or dopamine-resembling CVs generated by movement of an electrode was 0. These rates were calculated by measuring the distribution of *r* values for known dopamine signals (i.e., CVs recorded in vitro) and for known movement signals (i.e., CVs recorded during movement in vivo from probes that failed to detect any measurable dopamine) (*SI Materials and Methods*). Movement-related nondopamine CVs can display current changes at the redox potentials of dopamine and falsely correlate to dopamine standards. In this work, monkeys were capable of making moderate head movement as they were only fixed with a noninvasive side-clamp head restrainer (24) rather than a movement-resistant head-post. The head restrainer was chosen to reduce long-term risks associated with implanted head-posts. Therefore, the aforementioned procedures were critical to thoroughly remove signals that falsely allude to dopamine.

Automated Dopamine Detection. We automated detection of putative dopamine signals by constructing a template-matching algorithm (Fig. 3*A*). The script iteratively generates background-subtracted data to search for CVs correlated with dopamine standards with $r > r_t$ and $Q < Q_\alpha$. Background subtraction occurs at intervals of 10 samples to create a searchable scan window of data ±50 s from the background subtraction sample. In this background-subtracted scan window, the script iteratively searches for matching CVs at intervals of 0.5 s. When correlated samples are found, the script converts the current to $\Delta[DA]_a$ and searches for a time point (t_{max}) of local maximum of dopamine change around the correlated CV time point. When this local peak is found, the script searches for its rising and falling amplitudes having >2–5 nM (or equivalently, four to five times the root mean square of a 1-s period of the background signal) deflections around the $\Delta[DA]_a$ at t_{max}. If a peak ±0.7 s within the current peak has already been stored, or the current peak does not display adequate decreases ±2 s around itself, the signal is omitted. The CV at t_{max} is checked against standards ($r > r_t$ and $Q < Q_\alpha$). If CV(t_{max}) does not meet the criteria for dopamine identification, CVs ± 1 s around the peak are evaluated for dopamine identification. If these searches fail to provide a matching dopamine CV, the signal is omitted; otherwise, t_{max}, $\Delta[DA]_a$, and CV(t_{max}) are stored. This coarse detection scheme could be applied to continuous data (minutes to hours) recorded before and after drug modification to estimate changes in frequency of endogenous dopamine release. The reliability of these procedures is demonstrated in examples of detected CVs compared with in vitro standards, as shown in Fig. 3*B*, and in their reproducible application in detecting them with increased frequency following raclopride drug administration as corroborated in both acute and chronic measurements (Fig. 4, Fig. S4, and Table S1). In the context of this report, we define these local increases in apparent dopamine concentration as dopamine transients.

Drug Modulation. Raclopride (R-121, 0.05–0.1 mg/kg; Sigma-Aldrich) was administered intramuscularly to the monkeys to amplify stimulation-induced dopamine or endogenous dopamine neurotransmission. This drug has been shown to amplify electrically stimulated dopamine (20, 21) in rodents, as we confirmed in the primate (Fig. 2 and Fig. S3). Raclopride selectively binds to dopamine D2 receptors, and the inhibition of these receptors increases the firing rate of dopamine-containing neurons that innervate striatum (25). Electrochemical measurements in rodents demonstrate that raclopride induces increased rates of endogenous dopamine release (26, 27). Raclopride produces minimal effect on the levels of other neurotransmitters, such as noradrenaline and serotonin (28). The drug is well-tolerated in humans at low doses, and its major side effects are drowsiness and akathisia at higher doses (29). We noticed

that monkeys sometimes appeared tired, fell asleep, or became restless, 30–60 min after administration. Raclopride was freshly prepared on the day of each experiment by dissolving it in 0.9% saline (1 mg/mL).

Plots of dopamine transient rates (Figs. 4 *C–F* and Figs. S4 and S5) were generated by binning the number of detected peak signals (see *Automated Dopamine Detection*) for each minute of recording. Next, χ^2 tests were performed on the average baseline rate (period before raclopride administration) and the average postraclopride rate using a sliding window of equal width to the baseline period with 1-min increments following raclopride administration. The *P* values generated by these sliding window measures of χ^2 significance are plotted as a dashed (significant increase) or dotted (significant decrease) curve in the rate plots (Fig. 4 *C* and *D* and Figs. S4 and S5*A*) to display periods of recording when the average transient rate significantly exceeds the baseline rate (e.g., lower *P* value). Detected transients were then binned according to their apparent peak dopamine concentration change to plot the average detected rates according to their different ranges of dopamine concentration change (Fig. 4 *C* and *D* and Figs. S4 and S5*B*). Average rates before and after raclopride were calculated for each experimental session and were plotted to demonstrate the reproducibility of the rate increases over many days (Fig. 4 *E* and *F*). Average drug-induced changes in all sessions and subjects are reported as mean increases and *P* values are generated using two-tailed *t* tests.

Reward-Biased Visual Saccades in 1DR Task. In one monkey (M2), we measured dopamine neurotransmission during task performance in the 1DR behavioral paradigm. In this eye-movement task, the monkey was trained to fixate on a central cue for 1–2 s, then to make a saccade toward a target that appears on the left or the right of the screen, and then to fixate the target for 1–2 s to receive a small reward or large reward. The left or right direction of the target was associated with a small or large reward in a given session and usually did not change for a given day's session, but could randomly change across sessions. A meal shake (Ensure, Plus Nutrition Shake Vanilla) diluted with 50% water was delivered through a spout in volumes of 0.3 and 2.8 mL for small and large rewards, respectively. The probability of a large reward trial was set to 25%. The intertrial interval (ITI) was set at a fixed value between 5 and 15 s for each session.

Trials (reward time point ± ITI) were selected for dopamine analysis if the trial retained at least 70% of its recorded CVs with $Q < Q_{\alpha}$. Periods displaying extraneous CVs within each trial were automatically omitted during analysis of dopamine concentration changes and blanked out (in gray) in the plotted data (Figs. S6*B* and S7) (see *Chemometric Analysis*). Trial-by-trial changes in dopamine (Figs. S6*B* and S7) were computed by background-subtraction to the fixation period to evaluate differences in measured dopamine between small and large reward trials (Fig. 5*G*). Maximum $\Delta[DA]_a$ for each trial was calculated by finding the peak $\Delta[DA]_a$ at any time following fixation period until 5-s postreward delivery. This large time window for finding maximum $\Delta[DA]_a$ was used to account for prolonged dynamics in task-related striatal dopamine signals that we frequently observed in the measurements in monkeys (Fig. 5 *A–D*) and that our group has previously observed in behaving rodents (1), but have yet to fully interpret.

Changes in Dopamine Detection over Time. No standard criteria exist to assess changes in dopamine measurement functionality of probes over time. Prior investigations indicate that the CF's intrinsic sensitivity to dopamine (nA/μM) over chronic usage is not significantly altered as evaluated by post-explant in vitro flow-cell measurements (2). These studies also demonstrated that the dopamine signal originating from the nucleus accumbens, in response to unexpected reward, does not significantly change over time as measured from the chronically implanted probe. We attempted to characterize changes in probe performance based on measurements of stimulated release. We observed a decrease in measured stimulated dopamine in monkey M1 (Fig. 2). These decreases, however, could be a consequence of physical migration of the stiff stimulating electrodes relative to targeted dopamine-containing cell bodies. We also characterized the probes based on their ability to detect correlated dopamine CVs. We observed a decrease in the rate of detected dopamine in M1 across sessions in one of the probes (cn1) ($P < 0.003$), but not in the other implanted probes (cn2 and cn3) (Fig. 4*E*). Three of the implanted probes in M2 showed increase across sessions (cl1, p6, and cl6) ($P < 0.05$), whereas one of the probes did not show significant change (Fig. 4*F*).

ACKNOWLEDGMENTS. The authors thank Drs. B. Averbeck and A. Mitz (National Institute of Mental Health), P. E. M. Phillips and S. B. Ng-Evans (University of Washington), and V. Lovic (University of Calgary) for their advice during initial fast-scan cyclic voltammetric implementations; C. Erickson, L. Stanwicks, A. Burgess, H. F. Hall, S. P. Shannon, and Dr. Y. Kubota (Massachusetts Institute of Technology) for help with animal care, MRI, and manuscript preparation; and Drs. R. Desimone and N. P. Bichot (Massachusetts Institute of Technology) and C. Gray and B. Goodell (Gray Matter Research) for help with chamber design. This work is supported by the National Institutes of Health, National Institute of Neurological Disorders and Stroke Grants R01 NS025529 (to A.M.G.) and F32 NS093897 (to H.N.S.); the Army Research Office Contract W911NF-16-1-0474 (to A.M.G.); the NIH National Institute of Biomedical Imaging and Bioengineering Grant R01 EB016101 (to R.L., A.M.G., and M.J.C.); William N. and Bernice E. Bumpus Foundation (A.M.G.); Robert Buxton; and John Wasserlein and Lucille Braun.

1. Howe MW, Tierney PL, Sandberg SG, Phillips PEM, Graybiel AM (2013) Prolonged dopamine signalling in striatum signals proximity and value of distant rewards. *Nature* 500:575–579.
2. Clark JJ, et al. (2010) Chronic microsensors for longitudinal, subsecond dopamine detection in behaving animals. *Nat Methods* 7:126–129.
3. Lemaire N, et al. (2012) Effects of dopamine depletion on LFP oscillations in striatum are task- and learning-dependent and selectively reversed by L-DOPA. *Proc Natl Acad Sci USA* 109:18126–18131.
4. Crittenden JR, Graybiel AM (2011) Basal ganglia disorders associated with imbalances in the striatal striosome and matrix compartments. *Front Neuroanat* 5:59.
5. Kishida KT, et al. (2016) Subsecond dopamine fluctuations in human striatum encode superposed error signals about actual and counterfactual reward. *Proc Natl Acad Sci USA* 113:200–205.
6. Schluter EW, Mitz AR, Cheer JF, Averbeck BB (2014) Real-time dopamine measurement in awake monkeys. *PLoS One* 9:e98692.
7. Min H-K, et al. (2016) Dopamine release in the nonhuman primate caudate and putamen depends upon site of stimulation in the subthalamic nucleus. *J Neurosci* 36:6022–6029.
8. Yoshimi K, Kumada S, Weitemier A, Jo T, Inoue M (2015) Reward-induced phasic dopamine release in the monkey ventral striatum and putamen. *PLoS One* 10:e0130443.
9. Kozai TDY, Jaquins-Gerstl AS, Vazquez AL, Michael AC, Cui XT (2015) Brain tissue responses to neural implants impact signal sensitivity and intervention strategies. *ACS Chem Neurosci* 6:48–67.
10. Takmakov P, et al. (2010) Carbon microelectrodes with a renewable surface. *Anal Chem* 82:2020–2028.
11. Spencer KC, et al. (2017) Characterization of mechanically matched hydrogel coatings to improve the biocompatibility of neural implants. *Sci Rep* 7:1952, and erratum (2017) 7:12812.
12. Feingold J, et al. (2012) A system for recording neural activity chronically and simultaneously from multiple cortical and subcortical regions in nonhuman primates. *J Neurophysiol* 107:1979–1995.
13. Schultz W (1986) Responses of midbrain dopamine neurons to behavioral trigger stimuli in the monkey. *J Neurophysiol* 56:1439–1461.
14. Rebec GV (1998) Real-time assessments of dopamine function during behavior: Single-unit recording, iontophoresis, and fast-scan cyclic voltammetry in awake, unrestrained rats. *Alcohol Clin Exp Res* 22:32–40.
15. Ljungberg T, Apicella P, Schultz W (1992) Responses of monkey dopamine neurons during learning of behavioral reactions. *J Neurophysiol* 67:145–163.
16. Lauwereyns J, Watanabe K, Coe B, Hikosaka O (2002) A neural correlate of response bias in monkey caudate nucleus. *Nature* 418:413–417.
17. Tobler PN, Fiorillo CD, Schultz W (2005) Adaptive coding of reward value by dopamine neurons. *Science* 307:1642–1645.
18. Biran R, Martin DC, Tresco PA (2007) The brain tissue response to implanted silicon microelectrode arrays is increased when the device is tethered to the skull. *J Biomed Mater Res A* 82:169–178.
19. Schwerdt HN, et al. (2017) Subcellular probes for neurochemical recording from multiple brain sites. *Lab Chip* 17:1104–1115.
20. Fox ME, et al. (2016) Cross-hemispheric dopamine projections have functional significance. *Proc Natl Acad Sci USA* 113:6985–6990.
21. Moquin KF, Michael AC (2011) An inverse correlation between the apparent rate of dopamine clearance and tonic autoinhibition in subdomains of the rat striatum: A possible role of transporter-mediated dopamine efflux. *J Neurochem* 117:133–142.
22. Lynd-Balta E, Haber SN (1994) The organization of midbrain projections to the striatum in the primate: Sensorimotor-related striatum versus ventral striatum. *Neuroscience* 59:625–640.
23. Keithley RB, Wightman RM (2011) Assessing principal component regression prediction of neurochemicals detected with fast-scan cyclic voltammetry. *ACS Chem Neurosci* 2:514–525.
24. Amemori S, Amemori K, Cantor ML, Graybiel AM (2015) A non-invasive head-holding device for chronic neural recordings in awake behaving monkeys. *J Neurosci Methods* 240:154–160.
25. Krabbe S, et al. (2015) Increased dopamine D2 receptor activity in the striatum alters the firing pattern of dopamine neurons in the ventral tegmental area. *Proc Natl Acad Sci USA* 112:E1498–E1506.
26. Cass WA, Gerhardt GA (1994) Direct in vivo evidence that D2 dopamine receptors can modulate dopamine uptake. *Neurosci Lett* 176:259–263.
27. Aragona BJ, et al. (2008) Preferential enhancement of dopamine transmission within the nucleus accumbens shell by cocaine is attributable to a direct increase in phasic dopamine release events. *J Neurosci* 28:8821–8831.
28. Ogren SO, Hall H, Köhler C, Magnusson O, Sjöstrand SE (1986) The selective dopamine D2 receptor antagonist raclopride discriminates between dopamine-mediated motor functions. *Psychopharmacology (Berl)* 90:287–294.
29. Farde L, von Bahr C, Wahlen A, Nilsson L, Widman M (1989) The new selective D2-dopamine receptor antagonist raclopride–Pharmacokinetics, safety and tolerability in healthy males. *Int Clin Psychopharmacol* 4:115–126.